Biotechnol Lett (2015) 37:2181–2191
DOI 10.1007/s10529-015-1894-1

ORIGINAL RESEARCH PAPER

One step bioconversion of waste precious metals into *Serratia* biofilm-immobilized catalyst for Cr(VI) reduction

P. Yong · W. Liu · Z. Zhang · D. Beauregard · M. L. Johns · L. E. Macaskie

Received: 28 April 2015 / Accepted: 16 June 2015 / Published online: 14 July 2015

Abstract
Objectives For reduction of Cr(VI) the Pd-catalyst is excellent but costly. The objectives were to prove the robustness of a *Serratia* biofilm as a support for biogenic Pd-nanoparticles and to fabricate effective catalyst from precious metal waste.
Results Nanoparticles (NPs) of palladium were immobilized on polyurethane reticulated foam and polypropylene supports via adhesive biofilm of a *Serratia* sp. The biofilm adhesion and cohesion strength were unaffected by palladization and catalytic biofilm integrity was also shown by magnetic resonance imaging. Biofilm-Pd and mixed precious metals on biofilm (biofilm-PM) reduced 5 mM Cr(VI) to Cr(III) when immobilized in a flow-through column reactor, at respective flow rates of 9 and 6 ml/h. The lower activity of the latter was attributed to fewer, larger, metal deposits on the bacteria. Activity was lost in each case at pH 7 but was restored by washing with 5 mM citrate solution or by exposure of columns to solution at pH 2, suggesting fouling by Cr(III) hydroxide product at neutral pH.
Conclusion A 'one pot' conversion of precious metal waste into new catalyst for waste decontamination was shown in a continuous flow system based on the use of *Serratia* biofilm to manufacture and support catalytic Pd-nanoparticles.

Keywords Biofilm · Catalyst · Chromate reduction · Palladium · Precious metals · *Serratia* sp.

P. Yong · L. E. Macaskie (✉)
School of Biosciences, University of Birmingham, Edgbaston, Birmingham B15 2TT, UK
e-mail: l.e.macaskie@bham.ac.uk

W. Liu · Z. Zhang
School of Chemical Engineering, University of Birmingham, Edgbaston, Birmingham B15 2TT, UK

D. Beauregard
Department of Chemical Engineering and Biotechnology, University of Cambridge, Cambridge CB2 3RA, UK

M. L. Johns
School of Mechanical and Chemical Engineering, University of Western Australia, 35 Stirling Highway, Crawley, WA 6009, Australia

List of symbols

- Δ Displacement propagator: probability distributions of displacement over a set observation time
- W Work (J) done by an applied force to detach biofilm from the support

Introduction

Precious metal (PM)-based catalysts are widely used as industrial catalysts but concerns about their high

production costs and the need for stable nanoparticulate catalysts for high activity have led to the recognition of biogenesis as a means to synthesise precious metal-nanoparticles (NPs) supported on bacteria (Deplanche et al. 2011; de Corte et al. 2012). Bio-Pd-NP catalysts combine the benefits of homogeneous and heterogeneous catalysis (Creamer et al. 2007) with the stabilization of the Pd-NPs against agglomeration and permit their re-use without attrition or loss (Bennett et al. 2013). However free bacteria require encapsulation for use within columns. Granularized self-adhered biomass can immobilize catalytic Pd-nanoparticles (Suja et al. 2014) but granules (in a similar way to gel-encapsulation) may have low permeation properties.

Reduction of Cr(VI) by 'bio-Pd' has been well-reported (e.g. Mabbett et al. 2006; Humphries et al. 2006; Chidambaram et al. 2010; Deplanche et al. 2014) and defined Pd-nanocatalyst immobilized on a paradigm *Serratia* biofilm on a reticulated foam matrix functioned in the continuous reduction of Cr(VI) (Beauregard et al. 2010), a problematic environmental contaminant produced by various industries.

Application of PM catalysts per se to waste decontamination is not probably cost-effective. However PMs can be bio-refined from wastes into new catalytic materials (e.g. reviews by Macaskie et al. 2011; Deplanche et al. 2011; De Corte et al. 2012), the activity of which can be comparable to (or exceed) that of pure metal catalysts (Mabbett et al. 2006; Yong et al. 2010; Macaskie et al. 2011; Murray et al. 2015).

The first aim of this study was to confirm the robustness of the *Serratia* biofilm before and after formation of Pd-NPs (biofilm-Pd) and while reducing Cr(VI) under continuous-flow. The objective was then to compare the activity of a flow-through biofilm-Pd reactor in the reduction of Cr(VI) with that containing a mixed precious metal catalyst (biofilm-PM) made from an industrial processing waste. Such an immobilized catalyst could pave the way for making an inexpensive catalyst from one waste to remediate another.

Materials and methods

Biofilm growth and preparation of 'palladized' cells and biofilms

Serratia sp NCIMB 40259 was grown continuously in a 2.5 l air-lift fermenter under carbon (lactose)-limitation (Macaskie et al. 2005; Beauregard et al. 2010), with up to 240 washed polyurethane-reticulated foam (RF) discs [diameter (d) 2 cm; height (h) 0.45 cm, "TM30"; supplied by Recticel, Belgium] threaded on cotton strings secured within the vessel (sideways-on to the up-flow). The culture was maintained at steady-state ($D = 0.1$/h; 7 days) then the biofilm-foam discs [each $\sim$8.5 mg dried biomass as calculated from the OD_{600} of biomass suspension squeezed from the foam; biomass/dry weight conversion was as described by Mabbett et al. (2006)] were withdrawn into a sealed vessel over saline (4 °C, in air) until use. For biofilm growth on polypropylene (PP) discs the fermentation was in a 250 ml air-lift fermenter (identical aspect ratio to the 2.5 l vessel) with 50 discs cut from a PP container [$d = 2.0$ cm; $h = 0.1$ cm; un-sanded or sanded (Grade 0 sandpaper, Roebuck, UK; 100 strokes each)] as above (21 days). Each PP disc contained $\sim$6.2 and $\sim$7.7 mg dry biomass for unsanded and sanded discs, respectively (determined by scraping the material from the discs and estimation via OD_{600} after cell resuspension). Culture outflow (planktonic cells) was retained (between 2 and 7 days), harvested by centrifugation and washed in isotonic saline (8.5 g NaCl/l) twice.

For palladization planktonic cells were resuspended at an appropriate OD_{600} in 10 mM HNO_3 containing 2 mM Na_2PdCl_4 [to 25 % (w/w) Pd: dry biomass, i.e. 3 parts by mass of bacteria to 1 part by mass of Pd], left to stand [2 h; for biosorption of Pd(II)] and H_2 was bubbled through (15 min). Black 'bio-Pd' (gravity-settlement, overnight) was harvested by centrifugation, washed with water and processed for electron microscopy. All of the Pd(II) was removed as determined by assay of residual solution (Mabbett et al. 2006). For mixed precious metal catalyst from waste the same procedure was followed except that, in lieu of 2 mM Pd(II) solution, the cells were suspended in an industrial reprocessing waste [supplied with some compositional details by Degussa Ltd, Germany and supplemented with laboratory Pd(II) waste solution to mask the exact composition (Mabbett et al. 2006)] which was diluted 500-fold in water (pH was adjusted to 2.3). The final composition of the diluted waste was (mM) Pt, 2.8, Rh 0.14 (manufacturer's data) and total Pd, 1.9 [manufacturer's data plus additional known laboratory supplement (Mabbett et al. 2006)]. Preparation of biofilm-Pd PP discs (unsanded and sanded discs with biofilm) was done similarly, by immersion of the disc in the Pd solution (to the same loading of Pd

as for the free cells). For preparation of biofilm-Pd on reticulated foam (RF) discs a glass column stoppered at each end charged with seven biofilm-coated foam discs without (controls) or with 2 mM Pd(II) solution as above was filled with 7 ml (column fluid volume) allowed to stand (>2 h) then H_2 was introduced into the column (~10 min). The solution was drained and discarded Pd(II) was fully reduced and retained as Pd(0) (as above). This procedure was repeated until the loaded Pd(0) was 10 % of the biomass dry weight (w/w) [or 25 % (w/w) for electron microscopy]. For waste-precious metal-loaded biofilm columns (biofilm-PM), the processing waste was used in lieu of 2 mM Pd(II) solution, except that H_2 was put in the column for >30 min to ensure the metal ions were fully reduced (confirmed by assay as above; Rh was ignored as this component was small). The procedure was repeated until it was calculated that 10 % (w/w) ratio of PM (in total): biomass was achieved.

Examination of samples by electron microscopy

Planktonic cells or biofilms on PP discs and RF discs with (25 wt% Pd(0) or PM) or without added metals were fixed with 2.5 % (v/v) glutaraldehyde (in 0.1 M sodium cacodylate/HCl buffer pH 5.2; 4 °C; 1 h). For scanning electron microscopy samples were dehydrated at ambient temperature, carbon-coated and examined using an environmental scanning electron microscope (ESEM: FEI Philips FEG ESEM XL30) in high vacuum mode (Macaskie et al. 2005). For transmission electron microscopy (TEM) free cells with [25 % (w/w) metal] or without Pd/PM were fixed as above, stained, embedded and sectioned and the sections were placed onto a copper grid and viewed under a JEOL 1200CX2 TEM (Mikheenko et al. 2008). Bio-manufactured Pd was confirmed by energy dispersive X-ray microanalysis and confirmed as Pd(0) by X-ray powder diffraction as described previously (Deplanche et al. 2010; Bennett et al. 2013) by comparison of the obtained XRD pattern with references in the Joint Committee for Powder Diffraction Studies (JCPDS) data base.

Determination of biofilm adhesion and cohesion strength before and after palladization

Biofilm-coated PP discs were examined before and after 'palladization' (as above). The adhesive and cohesive strength of biofilm on the PP discs was measured using a micro-manipulation technique (Chen et al. 2005) using a sensitive force transducer (10 g, Kulite, USA). The force required to remove the biofilm away from the substrate at a speed of 1.1 mm/s versus sample time was measured, and the obtained data were used to calculate the adhesive strength, defined as the work done by the applied force F(t) per unit area of the biofilm (Chen et al. 2005). Hence the total work, W (J) done by the applied force, F(t), to detach biofilm from the support may be calculated as the integral of:

$$dW = Fdx \quad (1)$$

where the distance dx is vdt, so that

$$W = \frac{d}{(tC - tA)} \int_{t_A}^{t_C} Fdt \quad (2)$$

where d is the diameter of the circular disc, and t_A and t_C the first and last times at which the probe touched the biofilm surface. The apparent adhesive strength of a biofilm sample, σ (J/m^2), defined as the work (W) required to remove the sample per unit area (A) from the surface, is then given by: $\sigma = W/A$, assuming complete coverage of the disc surface by biofilm, which was confirmed by electron microscopy.

Examination of immobilized cell discs and columns using magnetic resonance imaging

Non-invasive magnetic resonance imaging (MRI) was used to visualize the biofilm coating on foam discs in a cylindrical flow cell (columns as above). Images were acquired using a Bruker DMX spectrometer featuring a 4.7 T vertical-bore super-conducting magnet using a ^1H (detected exclusively) resonance frequency of 200.17 MHz. 3D images of the reticulated foam flow cell were acquired with an isotropic resolution of 140 μm using the RARE imaging pulse sequence (Henning et al. 1986). This employed a recovery time of 2.5 s, an echo time of 6.8 ms and a RARE factor of 64. 2D velocity images were acquired using standard spin-echo imaging supplemented with pulsed field gradients (using gradients of 0.5 and 10 G cm^{-1}). This employed a 2 mm slice thickness and a 330 μm in-plane resolution. Displacement propagators were also acquired using the bipolar pulsed field gradient technique (Cotts et al. 1989). Displacement

propagators are probability distributions of displacement over a set observation time, Δ; in measurements here a value of 500 ms was employed. In this work this measurement is used to consider variations in velocity (displacement Δ^{-1}) before and after inclusion of biofilm and biofilm-Pd into the flow cell.

Cr(VI) reduction by biofilm-Pd and biofilm-PM in a flow-through reactor

Glass columns containing seven biofilm-Pd or biofilm-PM-coated foam discs [made from Pd(II) solution or metal waste, respectively] were challenged (up-flow) with solutions containing 0.5 mM $NaCrO_4$ and 25 mM sodium formate [electron donor for Cr(VI) reduction] under three conditions: (i) in 10 mM HCl (pH 2); (ii) in 20 mM MOPS/NaOH buffer (pH 7) or (iii) in 20 mM MOPS/NaOH buffer (pH 7) with, where stated, 5 mM citrate buffer pH 7 [to chelate liberated Cr(III) and minimize precipitation of $Cr(OH)_3$ in the reactor]. Columns and solutions were degassed with O_2-free N_2 (15 min) before filling the columns with solutions (i,ii or iii as above) and standing overnight. Cr(VI) solutions were then pumped upwards through the columns [bed vol 10 ml; flow rate (F) of 6 or 9 ml/h or as indicated]. Outflow samples were assayed for residual Cr(VI) using diphenylcarbazide (Mabbett et al. 2006). A previous mass balance of bio-Pd-catalyzed Cr(VI) reduction accounted for removed Cr(VI) as Cr(III) (Mabbett et al. 2006) and the Cr-speciation was confirmed in the *Serratia* biofilm-Pd column system by MRI (Beauregard et al. 2010). All experiments were done twice using independent bioPd preparations i.e. made from two separate fermentations; the reproducibility was within 5 % throughout.

Results and discussion

Formation of metallic-nanoparticles on free cells and biofilms

To visualize palladium-nanoparticle (Pd-NP) deposition, free cells from the fermenter outflow were initially examined. ESEM shows control cells with no surface features (Fig. 1a) whereas Pd-challenged cells bore nodules (~50 nm) on the cells (Fig. 1b), while TEM of a cell section (Fig. 1c) shows cell-bound nanoparticles, similar to those reported previously on cells of *E. coli* (Deplanche et al. 2010, 2014) and *D. desulfuricans* (Deplanche et al. 2014) and comprising palladium metal, shown by energy dispersive X-ray microanalysis, and identified as Pd(0) by X-ray powder diffraction, where the peaks corresponded to those for Pd(0) in the JCPDS database (results were as described for *E. coli* in Deplanche et al. 2010).

In Gram-negative fermentative bacteria the method of Pd-NP catalyst manufacture involves coordination of Pd(II) ions to cellular functional groups followed by hydrogenase-mediated reduction to Pd(0) into supported Pd-NPs (Mikheenko et al. 2008; Deplanche et al. 2010). Aerobically-grown cells [i.e. not expressing hydrogenases, although one has been described in *Salmonella* by Parkin et al. (2012)] of *E. coli* (Foulkes et al. 2011) and aerobically-grown *Serratia* sp. (Deplanche et al. 2014) also deposited catalytically-active Pd-NPs but the aerobic mechanism(s) of biogenesis is not known. The mechanism of Pd(0) deposition by the cells grown in the air-lift fermenter requires confirmation but this accords with Pd(0) formation by aerobically grown *E. coli* (Foulkes et al. 2011) and also with the observed reduction of Pd(II) by a hydrogenase-deficient *E. coli* mutant (Deplanche et al. 2010).

Planktonic cells were challenged with the PM waste in lieu of Pd(II) solution. The concentration of Pd(II) was 1.9 mM with a further ~3 mM contributed by Pt and Rh, giving a total of ~5 mM soluble PMs. While cells challenged with Pd(II) alone showed discrete Pd-NPs, evenly dispersed (Fig. 1c), cells challenged with the metal mixture showed fewer, much larger deposits (Fig. 1d). A detailed analysis of the NPs was not done but a previous study (Mabbett et al. 2006) used proton induced X-ray emission analysis of corresponding precious metal-nanoparticles (PM-NPs) on *D. desulfuricans* to establish the metal content as (by mass) 17 % Pt, 33 % Pd, 5.5 % Ag, 2.7 % Mg and 41.8 % Al, i.e. approximately equimolar Pd and Pt with some Ag on a 'carrier' of Al and it was assumed that the NPs on *Serratia* were of similar composition.

Figure 1e shows a SEM image of native biofilm on a polypropylene (PP) disc, with individual cells apparent, crosslinked and intermeshed by strands of dehydrated, collapsed extracellular polymeric materials (EPM) (Fig. 1e; inset). It was not possible to differentiate between collapsed EPM, pili or indeed curli, amyloid structures protruding from cell surfaces

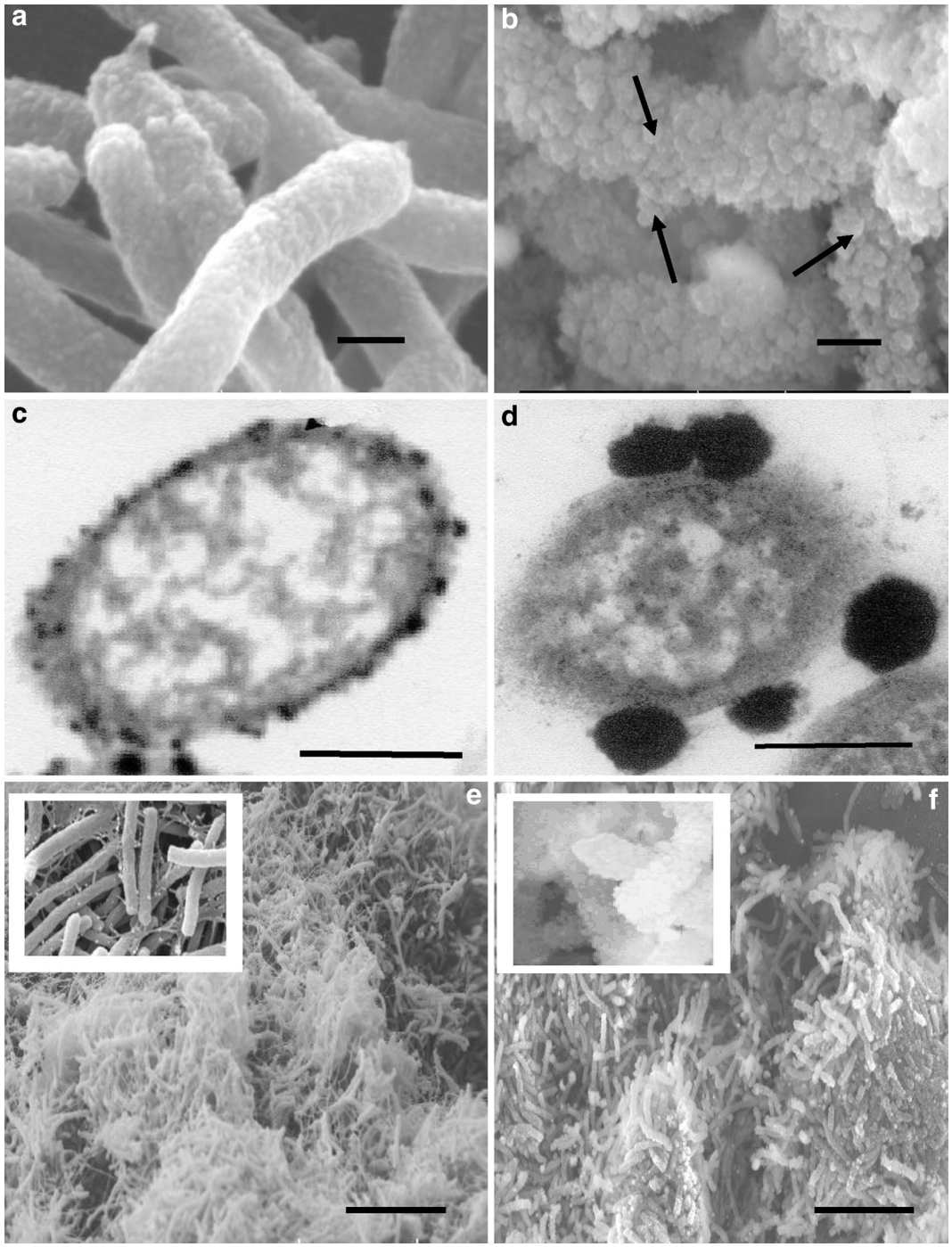

as a tangled matrix which play a role in biofilm formation (Bokranz et al. 2005). On deposition of Pd(0) the biofilm was better defined (Fig. 1f), with a nodular appearance of individual cells (Fig. 1f, inset) similar to the planktonic cells (Fig. 1b. Similar results were obtained using biofilm immobilized on reticulated foam (not shown). The higher definition can be attributed to the crosslinkage and shrinkage of the

◀**Fig. 1** Localization of Pd deposits on *Serratia* cells visualized by electron microscopy. **a** and **b** SEM images under ESEM (high vacuum mode; planktonic cells) of cells before (**a**) and following **b** palladization (25 % of the bacterial dry weight as described in "Materials and Methods" section). *Bars* are 500 nm. **c** TEM of a single cell showing deposited palladium nanoparticles. **d** Corresponding cell treated with industrial precious metal processing waste. *Bars* are 500 nm. **e**, **f** Biofilm on the surface of a polypropylene disc without (**e**) or with (**f**) metallic palladium deposits ('biofilm-Pd') 25 % of biomass dried weight, w/w) examined under ESEM (high vacuum mode after carbon coating). Note that the cells appear to be crosslinked by collapsed EPM strands in the absence of Pd deposits (Fig. 1e, *inset*) but in the palladized biofilm the residual crosslinking strands appear to be absent while the cells have a nodulated appearance as in Fig. 1b. (Figure 1f and *inset*). *Bars* are 10 μm. The nodules were confirmed as Pd using energy dispersive X-ray microanalysis and as Pd(0) by X-ray powder diffraction (not shown)

EPM strands by metal cations into well-defined, compacted structures surrounding the cells (Macaskie et al. 2000).

The planktonic cells were taken from the air-lift culture outflow. However since the O_2 gradient was not measured in the biofilm the participation of hydrogenases in a proportion of cells within an anaerobic niche cannot be ruled out. Hydrogenase upregulation occurs during shift into anaerobiosis; even a few seconds is sufficient to induce genes of anaerobic pathways (Schweder et al. 1999). A heterogeneous environment due to insufficient mixing would be more pronounced in a three-phase (gas, liquid, solid) biofilm system. In addition, biofilms function as a significant reservoir of potential planktonic cells arising via controlled cell detachment (Bester et al. 2005). Hence the planktonic fraction may have contained cells arising from the biofilm via turnover. For these reasons, a direct comparison between planktonic and biofilm-cells is not trivial and was not attempted but Fig. 1 shows that the Pd deposition on biofilm-cells was similar to their planktonic counterparts.

Robustness of biofilms with and without Pd

Initial tests using fluorescent dye showed that the biofilm adhered tightly to the glass surface of the fermenter under a water jet. Biofilm-columns must function under a continuous flow for extended periods, hence robustness is essential. A study using *E. coli* showed that, while biofilm formed under the conditions described here, it detached from the support within a few days (C. Mennan and L.E. Macaskie, unpublished work). The *Serratia* biofilm maintained integrity but this has not been quantified previously. Several authors have described the mechanical properties of biofilm but results are difficult to compare as different techniques were used; mechanical parameters have been described in terms of shear strength (Poppele and Hozalski 2003; Mohle et al. 2007) tensile strength and elastic modulus (Stoodley et al. 1999). In this study, the biofilm adhesion and cohesion strength was estimated using a micromanipulation method (Chen et al. 2005; Liu et al. 2006) (Table 1). Roughening the support approximately doubled the work needed to detach the fresh biofilm but made little difference after palladization. Using unsanded disc the adhesion and cohesion strength were the same within experimental error before and after palladization (Table 1). The adhesion tests were carried out using polypropylene discs (since these could be roughened). Similar results were obtained using glass microscope slides (not shown).

The appearance of reticulated foam (RF) discs is shown in Fig. 2a and b; the latter shows clearly the biofilm layer on the foam mesh which appears dark in MRI (Fig. 2 d) due to the lower water content of biomass as compared to interstitial water. Figure 2c shows 2-dimensional slices extracted from 3D high resolution MRI images of foam columns before and after inclusion of *Serratia* biofilm and Pd. The structure of the foam is evident (Fig. 2c, left). Addition of the *Serratia* and the Pd result in localized signal loss (Fig. 2d), predominately due to a reduction in T_2 signal relaxation. To examine for blockages (due to dislodged biofilm) 2D MRI velocity maps were

Table 1 The adhesion and cohesion strength of Pd-biofilm on polypropylene discs

Biofilm support	Work done to detach the biofilm (J/m^2)	
	Native biofilm	Pd-biofilm
PP unsanded disc	1.76 ± 0.31	1.37 ± 0.22
PP unsanded disc	3.36 ± 0.75	1.71 ± 0.19

Biomass adhesion and cohesion strength was measured using a manipulation technique and presented as work-done per unit area (J/m^2) to detach the biofilm from the supporting surfaces (mean ± standard deviation, $n \geq 3$), as described in "Materials and Methods" section

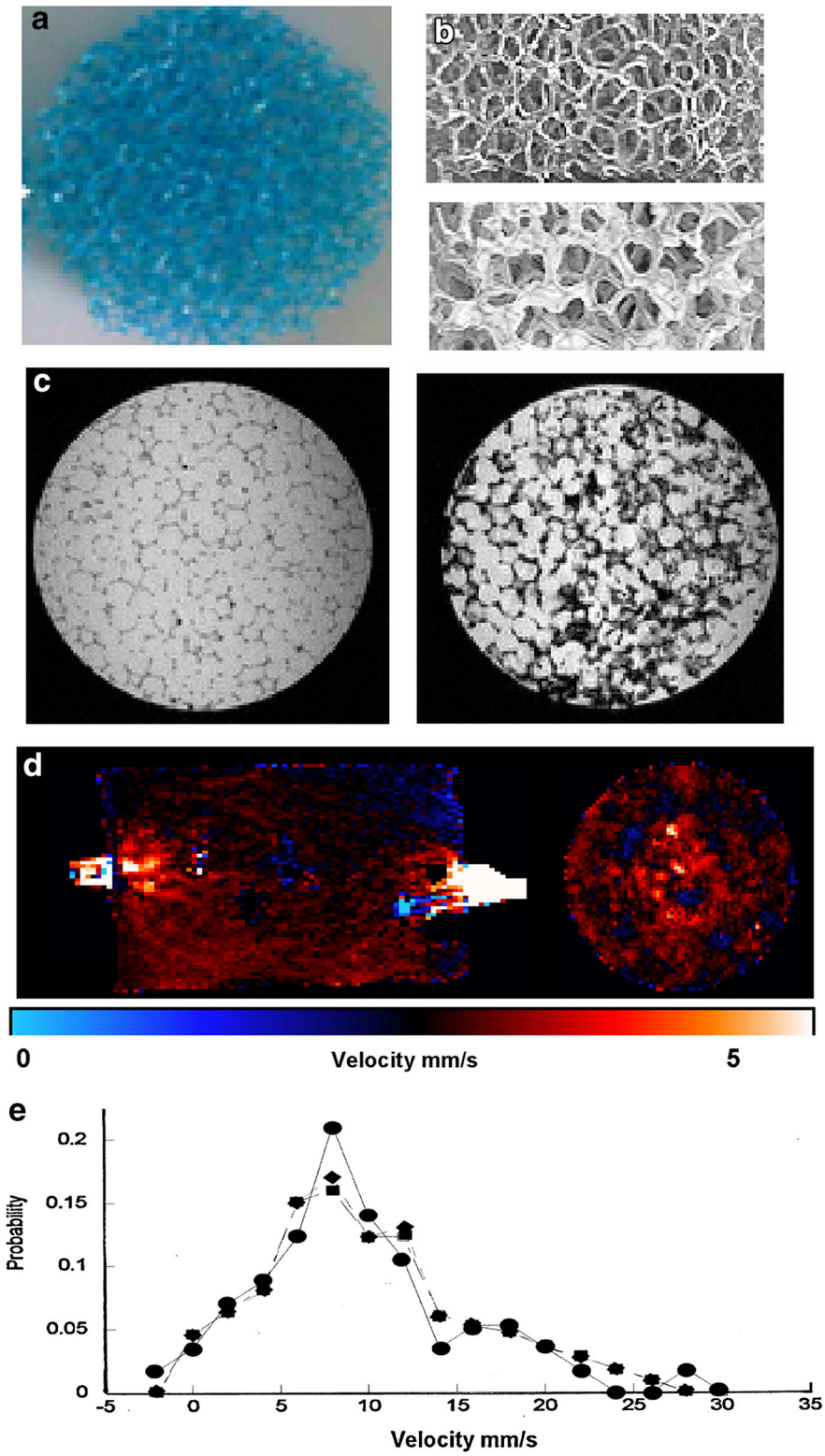

Fig. 2 Examination of catalyst material by magnetic resonance imaging **a** Reticulated foam disc (2 cm diameter × 0.5 cm height) before biofilm formation. **b** Portion of foam (1 cm × 0.5 cm) before (*top*) and after (*bottom*) biofilm formation. **c** Slices from 3D MRI images for the columns packed with 2 cm diameter foam discs; before (*left*) and after (*right*) formation of biofilm and Pd deposition. **d** 2D velocity images acquired from a column packed with foam discs with biofilm and Pd. The velocity component in the superficial flow direction is shown for slices parallel and perpendicular to the column axis. **e** Propagators (expressed as velocity probability distributions) for the column packing for fresh foam (*filled circle*) and with inclusion of biofilm (*filled square*) and biofilm-Pd (*filled diamond*) respectively

recorded of the biofilm-Pd foam flow cell in two orthogonal directions (Fig. 2d). Whilst the flow was not homogeneous, and entrance/exit effects (higher velocity channels) are evident, there was no evidence of any substantial blockage of the pore space. Such 2D images only capture information from a portion of the column defined by the slice thickness employed. To explore variations in flow field more thoroughly, displacement propagators were acquired as shown in Fig. 2e for the foam, foam + biofilm and foam + biofilm-Pd samples as probability distributions of velocity (Displacement Δ^{-1}). No increase in stagnant flow was evident as shown by the probability distributions as a consequence of the treatment. Figure 2e shows a slight shift to higher velocities following treatment, indicative of a slight, expected reduction in system porosity as part of the void space around the foam struts becomes occluded with the biofilm. An identical result for the native and palladized biofilm was obtained, suggesting that the increased thickness of each cell due to its Pd-layer (Fig. 1a,b) is counterbalanced by contraction of the biomaterial upon mineralization as suggested in Fig. 1e,f.

Reduction of Cr(VI) catalysed by bio-Pd and palladized biofilms

Neither planktonic cells nor biofilms reduced Cr(VI) in the absence of Pd(0). Biofilm-Pd coated RF discs were challenged with Cr(VI) in flow-through columns (Fig. 3). In accordance with the strong biofilm adhesion (above) no biofilm or Pd was detected in column exit flows. At pH 2 (Fig. 3a) at a flow rate (F) = 12 ml/h Cr(VI) was removed continuously. At higher flow rates (15 and 18 ml/h) some activity was lost after ~2 bed volumes (Fig. 3a). In contrast at pH 7 (Fig. 3b) activity was lost after only ~1 bed volume at 9 ml/h but this was mitigated by addition of 5 mM citrate [which chelates Cr(III) product and suppresses formation of $Cr(OH)_3$]. Citrate was not required at pH 2 even at higher flow rates (Fig. 3a) and the inhibition at pH 7 was attributed to fouling with nascent colloidal Cr(III) hydroxide.

Mabbett et al. (2006) concluded, from mass balance data, and in line with other authors, that loss of Cr(VI) equated to its reduction to Cr(III). Although this *Serratia* sp. has high phosphatase activity when grown under these conditions (Macaskie et al. 2005), it proved impossible to remove Cr(III) by precipitation as its phosphate via this enzymatic route; indeed, addition of excess PO_4^{3-} ions to Cr^{3+} in vitro gave no $CrPO_4$; hence precipitation of Cr(III) as its phosphate within the column could be discounted, especially since no exogenous phosphorus source was provided. Tests using ^{31}P MRI to check for liberation of phosphate and possible formation of a soluble species of chromium phosphate were inconclusive, attributed to the low sensitivity of MR techniques to P as compared to protons and its relatively low concentration in the columns.

The above tests confirm this biofilm system as a stable immobilized catalyst. Next, the use of precious metals sourced from a commercial waste was tested. Industrial waste compositions are typically confidential and commercially-sensitive (as details of the parent process could be back-calculated). As a condition of its provision, no detailed analysis was carried out on the waste solution (concentrations of key metals were provided by the supplier) and its composition was masked with additional waste Pd(II) from laboratory stock to the concentration shown (Mabbett et al. 2006). This study was designed to confirm that, in principle, a waste source is compatible with a biofilm-system. Wastes will vary substantially between and even within industrial sources as processing technologies evolve; materials may vary even within one operation and hence each study using a waste as a resource is unique.

The activity of biofilm-PM columns is shown in Fig. 3c. Columns were tested at 6 ml/h. Without citrate only columns at pH 2 retained activity; at pH 7 without citrate activity was lost rapidly, as with Pd-catalyst (Fig. 3c). Citrate addition improved the removal of Cr(VI), with comparable activities [>95 % removal of Cr(VI)] between the biofilm-PM-columns held at 2/3 of the flow rate as their pure Pd(0) counterparts (Fig. 3c). The lost activity at pH 7 was attributable to the formation of a passivation layer of CrOOH which would coat the mineral surface and prevent further electron transfer to Cr(VI) (Manning et al. 2006). However >95 % Cr(VI) reduction was restored using biofilm-PM columns (F = 6 ml/h) when the inhibited column was 'rescued' with pH 2 solution following challenge at pH 7 for several days (not shown), i.e. Cr(VI) reduction done at pH 2 can reverse the inhibitory passivation. This is a positive factor for use in real Cr(VI) remediation processes as many industrial waste solutions are produced at low

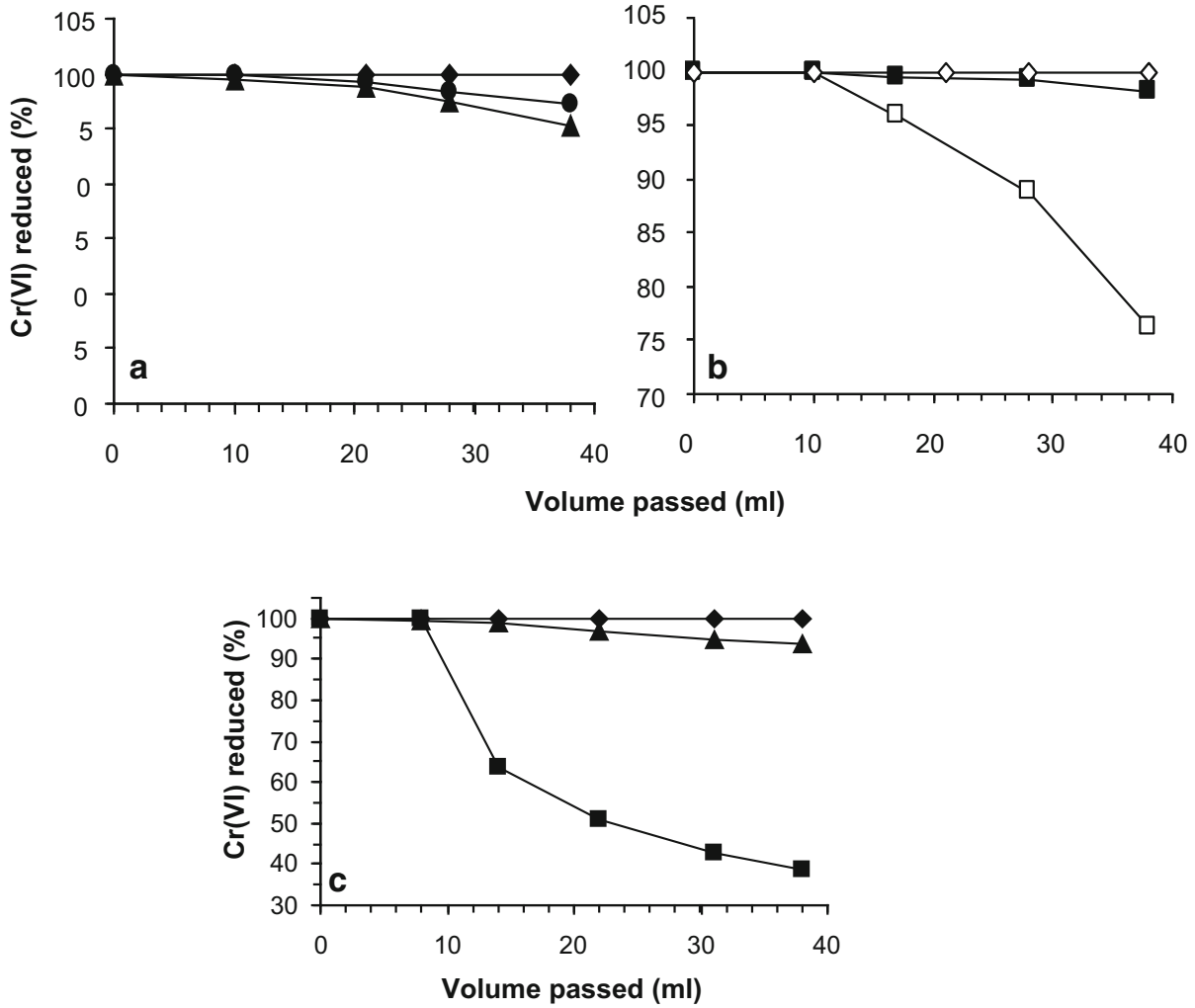

Fig. 3 Cr(VI) reduction in columns with seven biofilm immobilized-Pd or biofilm-PM discs. Columns were filled with degassed Cr(VI) solutions and left overnight and then solution was passed through the columns at various flow rates (F: ml/h). A control column with biofilm-foam discs (no palladium) gave no Cr(VI) reduction (not shown) at all conditions tested. Data are mean from two experiments; errors were within 5 %. *3a* Biofilm-Pd column challenged with pH 2 solution (no citrate) at flow rates of (ml/h): 12 (*filled diamond*); 15 (*filled circle*): 18 (*filled triangle*). *3b* Biofilm-Pd column challenged with pH 7 (no citrate) solution at flow rates of (ml/h) *open diamond*: 6; *open square*: 9, and supplemented with 5 mM citrate buffer at a flow rate of 9 ml/h (*filled square*). *3c* Biofilm-PM column challenged with various solutions at a flow rate of 6 ml/h as follows: *filled diamond* pH 2, no citrate; *filled square* pH 7, no citrate; *filled triangle* pH 7, with 5 mM citrate. All data are means from two experiments; *errors* were within 5 %

pH. Periodic 'refreshment' of the column at pH 2 overcomes the need and expense of adding citrate continuously, which would also add to the biological oxygen demand (BOD) of the final solution. At flow rates of 12 and 6 ml/h, respectively, the biofilm-Pd and biofilm-PM columns removed 95–100 % of 0.5 mM Cr(VI) continuously over 5 days with sustained activity (the longest times tested). Previous work using using *Serratia* biofilm-Pd in sequential experiments (Beauregard et al. 2010) showed that columns are stable over at least several weeks.

The biofilm-PM columns were approximately 66 % as active as the biofilm-Pd columns (6 and 9 ml/h respectively was required for complete removal of Cr(VI)). The underlying reason was not investigated but since the PM-NPs were fewer and larger (Fig. 1d; c.f. Fig. 1c) a simple surface area effect may be a sufficient explanation. The effect of Al as a 'diluent'

(Mabbett et al. 2006) is not known. A comparison of catalysts made using 'pure' Pd(II) and metal mixtures is made difficult using real waste sources, not only because of the differing metal compositions between samples but due to the co-presence of other agents. For example, Murray et al. (2015) found that the high catalytic activity seen in catalyst sourced from model waste solution (the PM content was based on real automotive catalyst leachate) was decreased by sourcing the metals from the real waste leachate; the inhibitory effect was mimicked by 'spiking' the model system with other components found in the real waste. On the other hand, metal mixtures from real wastes were sometimes found to enhance the catalytic activity as compared to using 'pure' metals (e.g. Yong et al. 2010).

In conclusion, this study shows the potential for biofilm-PM as an inexpensive remediation catalyst via strong biofilm adhesion to support materials. While reticulated foam has insufficient mechanical strength for large scale operation, various porous matrices for optimal biofilm support and activity have been the subject of numerous previous investigations (e.g. see Kafai 2011).

Acknowledgments This work was supported by the EPSRC (Grants No. EP/E0122213/1, EP/D05768X/1 and EP/1007806/1) and NERC (Grant No NE/L014076/1). We acknowledge, with thanks, the provision of polyurethane reticulated foam cubes (Filtren TM30) by Recticel, Belgium.

References

Beauregard DA, Yong P, Macaskie LE, Johns ML (2010) Using non-invasive magnetic resonance imaging (MRI) to assess the reduction of Cr(VI) using a biofilm-palladium catalysts. Biotechnol Bioeng 107:11–20

Bennett JA, Mikheenko IP, Deplanche K, Shannon IP, Wood J, Macaskie LE (2013) Nanoparticles of palladium supported on bacterial biomass; new, recyclable heterogeneous catalyst with comparable activity to homogeneous colloidal Pd in the Heck reaction. Appl Chem B 140–141:700–707

Bester E, Wolfaardt G, Joubert L, Garny K, Saftic S (2005) Planktonic cell yield of a *Pseudomonas* biofilm. Appl Environ Microbiol 71:7792–7798

Bokranz W, Wang X, Tschape H, Romling U (2005) Expression of cellulose and curli fimbriae by *Escherichia coli* from the gastrointestinal tract. J Med Microbiol 54:1171–1182

Chen MJ, Zhang Z, Bott TR (2005) Effects of operating conditions on the adhesive strength of *Pseudomonas fluorescens* biofilms in tubes. Colloids Surf B 43:61–71

Chidambaram D, Hennebel T, Taghavi S, Mast J, Boon N, Verstraete W, Van der Lelie D, Fitts JP (2010) Concomitant microbial generation of palladium nanoparticles and hydrogen to immobilize chromate. Environ Sci Technol 44:7635–7640

Cotts RM, Hoch MJR, Sun T, Markert JT (1989) Pulsed field gradients stimulated echo methods for improved NMR diffusion measurements in heterogeneous systems. J Magn Reson 83:252–260

Creamer NJ, Mikheenko IP, Yong P, Deplanche K, Sanyahumbi D, Wood J, Pollmann K, Merroun M, Selenska-Pobell S, Macaskie LE (2007) Novel supported Pd hydrogenation bionanocatalyst for hybrid homogeneous/heterogeneous catalysis. Catal Today 128:80–87

De Corte S, Hennebel T, de Gusseme B, Verstraete W, Boon N (2012) Bio-palladium: from metal recovery to catalytic applications. Microb Biotechnol 5:5–17

Deplanche K, Caldelari I, Sargent F, Macaskie LE (2010) Involvement of hydrogenases in the formation of highly catalytic Pd(0) nanoparticles by reduction of Pd(II) using *Escherichia coli* mutant strains. Microbiology 156:2630–2640

Deplanche K, Murray AJ, Mennan C, Taylor S, Macaskie LE (2011) Biorecycling of precious metals and rare earth elements. In: Rahman MM (ed) Nanomaterials, InTech Publications Intechweb.org, 2011. Chapter 12, pp 279–314

Deplanche K, Bennett JA, Mikheenko I, Omajali J, Wells A, Meadows R, Wood J, Macaskie LE (2014) Catalytic activity of biomass-supported Pd nanoparticles: influence of the biological component in catalytic efficacy and potential application in 'green' synthesis of platform chemicals. Appl Catal B 147:651–665

Foulkes JA, Malone J, Coker VS, Turner NJ, Lloyd JR (2011) Engineering a bimetallic whole cell catalyst for enantioselective deracemization reactions. ACS Catal 1:1589

Henning J, Nauerth A, Friedburg H (1986) RARE imaging—a fast imaging method for clinical MR. Magn Reson Med 3:823–833

Humphries AC, Mikheenko IP, Macaskie LE (2006) Chromate reduction by immobilized palladized sulfate-reducing bacteria. Biotechnol Bioeng 94:81–90

Kafai K (ed) (2011) Porous media applications in biological systems and biotechnology. CRC Press, Boca Raton

Liu W, Fryer PJ, Zhang Z, Zhao Q, Liu Y (2006) Identification of cohesive and adhesive effects in the cleaning of food fouling deposits. Innov Food Sci Emerg Technol 7:263–269

Mabbett AN, Sanyahumbi D, Yong P, Macaskie LE (2006) Biorecovered precious metals from waste automotive catalysts: single step conversion of liquid waste to bioinorganic catalyst with environmental application. Environ Sci Technol 40:1015–1021

Macaskie LE, Bonthrone KM, Yong P, Goddard DT (2000) Enzymically mediated bioprecipitation of uranium by a *Citrobacter* sp.: a concerted role for exocellular lipopolysaccharide and associated phosphatase in biomineral formation. Microbiology 146:1855–1867

Macaskie LE, Yong P, Thackray A, Sammons RL, Marquis PM (2005) A novel non line-of-sight method for coating hydroxyapatite onto the surfaces of support materials by biomineralization. J Biotechnol 118:187–200

Macaskie LE, Mikheenko IP, Yong P, Deplanche K, Murray AJ, Paterson-Beedle M, Coker VS, Pearce CI, Cutting R,

Pattrick RAD, Vaughan D, Van Der Laan G, Lloyd JR (2011) Today's wastes tomorrow's materials for environmental protection. In: Moo-Young M, Butler MC, Webb C, Moreira A Grodzinski B, Cui ZF, Agathos S (eds) Comprehensive biotechnology, vol 6, Elsevier, Amsterdam, ISBN 978-0-444-53353-4, pp 719–725

Manning BA, Kiser JR, Kanel SR (2006) Spectroscopic investigation of Cr(III) and Cr(VI)-treated nanoscale zerovalent iron. Environ Sci Technol 41:586–592

Mikheenko I, Rousset M, Dementin S, Macaskie LE (2008) Bioaccumulation of palladium by *Desulfovibrio fructosovorans* and hydrogenase deficient strains. Appl Environ Microbiol 19:6144–6146

Mohle RB, Langemann T, Haesner M, Augustin W, Scholl S, Neu T, Hempel DC, Horn H (2007) Structure and shear strength of microbial biofilms as determined with confocal laser scanning microscopy and fluid dynamic gauging using a novel rotating disc biofilm reactor. Biotechnol Bioeng 98:747–755

Murray AJ, Taylor SM, Zhu J, Wood J, Macaskie LE (2015) A novel biorefinery: biorecovery of precious metals from spent automotive catalyst leachates into new catalysts effective in metal reduction and in the hydrogenation of 2-pentyne. Min Eng (in press)

Parkin A, Bowman L, Roessler M, Davies RA, Palmer T, Armstrong F, Sargent F (2012) How *Salmonella* oxidises H_2 under aerobic conditions. FEBS Lett 586:536–544

Poppele EH, Hozalski RM (2003) Micro-cantilever method for measuring the tensile strength of biofilms and microbial flocs. J Microb Methods 55:607–615

Schweder T, Krüger E, Xu B, Jürgen B, Blomsten G, Enfors SO, Hecker M (1999) Monitoring of genes that respond to process-related stress in large-scale bioprocesses. Biotechnol Bioeng 31:579–586

Stoodley P, Lewandowski Z, Boyle JD, Lappin-Scott HM (1999) Structural deformation of bacterial biofilms caused by short-term fluctuations in fluid shear: an in situ investigation of biofilm rheology. Biotechnol Bioeng 65:83–92

Suja E, Nancharaiah YV, Venugopalan VP (2014) Biogenic nanopalladium production by self immobilized granular biomass: application for contaminant remediation. Water Res 65:395–401

Yong P, Mikheenko IP, Deplanche K, Redwood MD, Macaskie LE (2010) Biorefining of precious metals from wastes—an answer to manufacturing of cheap nanocatalysts for fuel cells and power generation via an integrated biorefinery? Biotechnol Lett 32:1821–1828